Available online at www.sciencedirect.com
SCIENCE DIRECT
Trans. Nonferrous Met. Soc. China 18(2008) 593−597
Transactions of Nonferrous Metals Society of China
www.csu.edu.cn/ysxb/

Phase selection of ternary intermetallic compounds during solidification of high zinc magnesium alloy

GUAN Shao-kang(关绍康)[1], ZHANG Chun-xiang(张春香)[1], WANG Li-guo(王利国)[1], WU Li-hong(吴立鸿)[1], CHEN Pei-lei(陈培磊)[1], TANG Ya-li(汤亚力)[2]

1. School of Materials Science and Engineering, Zhengzhou University, Zhengzhou 450002, China;
2. Materials Science Division, Argonne National Laboratory, Argonne, IL60439, USA

Received 18 May 2007; accepted 23 August 2007

Abstract: The phase selection of ternary intermetallic compound τ phase ($Mg_{32}(Al, Zn)_{49}$) and φ phase ($Al_2Mg_5Zn_2$) in high zinc magnesium alloys was studied by using scanning electron microscope, X-ray diffractometer and differential scanning calorimeter, etc. The results indicate that, when adding element Si in Mg-8Zn-4Al-0.3Mn (ZA84) alloy, φ phase is promoted, whereas τ phase is inhibited. The Chinese script-type Mg_2Si and matrix microstructure are greatly refined, the formation of τ phase is facilitated and φ phase is restrained when modifier Al-AlP master alloy is added in ZA84 alloy containing Si. The kinetics study of phase selection indicates that there is a critical degree of undercooling of the melt. If the undercooling exceeds the critical value, τ phase preferentially forms while φ phase is restrained; otherwise, φ phase preferentially forms while τ phase is restrained.

Key words: high-zinc magnesium alloy; Si; AlP; phase selection; kinetics

1 Introduction

During the past decade, magnesium alloys have been widely used in automobile and electronic industry because of their low density, high specific strength, good damping and electromagnetic shielding capacities, etc. At present, the Mg-Al alloys are most extensively used in automobile, such as AZ91 and AM60, but their properties steeply fall when the work temperature is over 393 K. High-zinc Mg alloys (zinc content over 5% in general, mass fraction) are newly developed heat-resistant alloys, and are strengthened mostly by ternary intermetallic compound τ phase ($Mg_{32}(Al, Zn)_{49}$, with good creep-resistant property) and a little φ phase($Al_2Mg_5Zn_2$). However, it is urgent to improve the castability of the alloys and its elevated-temperature mechanical properties. The resent study indicated that the fluidity of Mg-8Zn-4Al-0.3Mn (ZA84) alloy was remarkably improved for the addition of silicon[1−3], and the Chinese script-type Mg_2Si and microstructure were greatly refined when modifier Al-AlP master alloy was added in ZA84 containing Si[4−5]. During the alloying and modifying of the experimental alloys, the phase selection between the τ phase and φ phase occurred. The phase selection order of ternary intermetallic compounds will be mainly investigated in this work.

2 Experimental

The chemical compositions of three alloys are given in Table 1. The addition of AlP is calculated by P content. The alloys were prepared by using the following materials: commercial pure Mg, Al and Zn (＞99.9%), Al-50%Si, Al-6%AlP and Al-20%Mn master alloy. The melting was carried out in an electric resistance furnace and protected by JDRJ protectant. After being refined by JDMJ flux, the melt was poured into a steel mold (the size of test bars d25 mm×100 mm) preheated at 250 ℃. The microstructure was characterized by Olympus optical and JSM-5801LV scanning electron microscopy. The chemical compositions of the micro-region were determined by Oxford energy X-ray dispersive spectrometer attached to TEM. The phases of the alloys were identified by X-ray diffraction spectroscopy using

Foundation item: Project(50571092) supported by the National Natural Science Foundation of China; Project(0523020500) supported by the Excellent Young Scholars Foundation of Henan Province, China
Corresponding author: GUAN Shao-kang; Tel: +86-371-67781592; E-mail: zhangcx@zzu.edu.cn

Table 1 Composition of alloys (mass fraction, %)

Alloy	Mg	Zn	Al	Mn	Si	P
ZA84	Bal.	8.1	4.2	0.31	0	0
096Si	Bal.	8.05	4.06	0.28	0.96	0
01P	Bal.	7.92	3.93	0.29	1.13	0.01

Cu K_α radiation. The solidification process of the alloys was analyzed by Labsys DSC(Differential Scanning Calorimetry) at heating rate of 5 K/min.

3 Results and discussion

3.1 Phase selection of ternary intermetallic compounds in alloys

The XRD patterns (Fig.1) show that τ is the main ternary intermetallic in ZA84 alloy, in which a little of φ exists; in 096Si alloy, φ is the main ternary intermetallic, while τ is little. These reveal that the addition of Si in ZA84 alloy facilitates the formation of φ phase, while restrains the formation of τ phase. Fig.1(c) shows that τ is the main ternary intermetallic, only a little of φ exists in 01P alloy, which indicates that τ phase is promoted while φ phase is inhibited when AlP is added in 096Si alloy. All these indicate that the additions of Si or Si and AlP result in the phase selection(the preferential precipitation sequence of competing phases) between τ and φ in ZA84 alloy.

Fig.2 shows the SEM morphologies of the alloys. The chemical composition of the phases in Fig.2 is given in Table 2. Fig.2(a) (ZA84 alloy) shows that the bone-type τ phase distributes along grain boundary; in Fig.2(b) (096Si alloy), the bone-type phase is φ and there is beehive or fish-bone loose microstructure in φ, which indicates φ phase is more dispersive than τ phase. Moreover, there is Chinese script-type Mg_2Si phase in 096Si alloy. Fig.2(c) (01P alloy) shows the compact τ phase as well as the refined microstructure. The SEM images verify the phase selection between τ and φ due to the additions of Si, also the addition of Si and AlP in ZA84.

3.2 DSC analysis on solidification process of alloys

Fig.3 shows the heating DSC curves of ZA84, 096Si and 01P alloys. The present interpretation of these thermal curves is based on the Mg-Zn-Al ternary diagram[6−7], since the Mg-Zn-Al-Si phase diagram is not available. This procedure is justified by the fact that a minor amount of Si is introduced in ZA84 alloy and Si does not take part in the reactions of ternary phase (τ and φ). The first thermal valley of DSC curves in Fig.3 is the reaction, in which τ or φ forms, and the second corresponds to the α(Mg) reaction. The characteristic temperature values of the alloys are listed in Table 3.

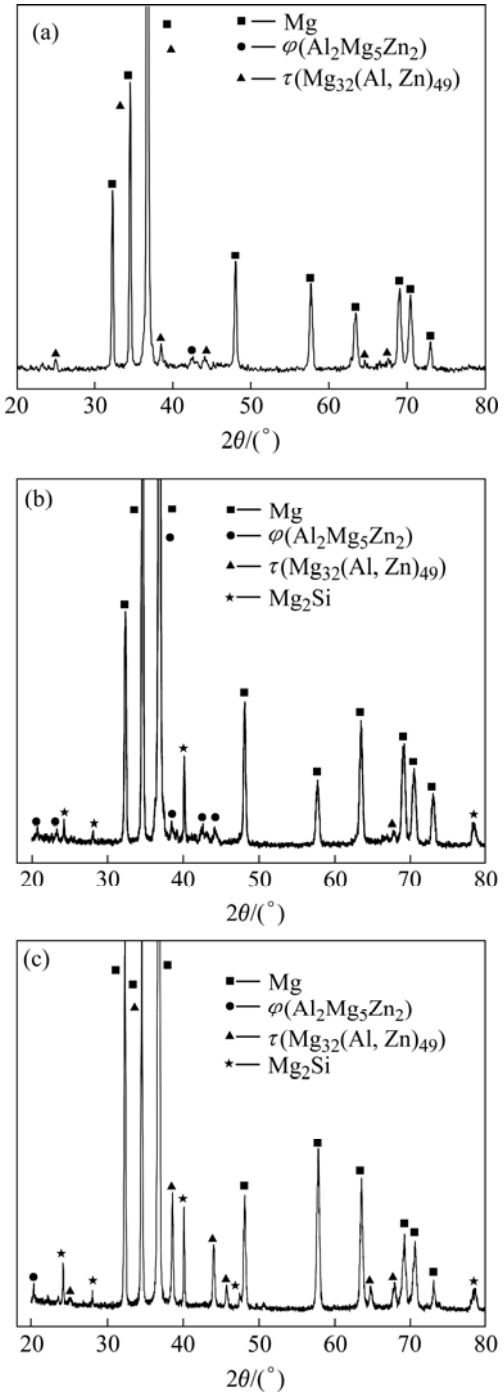

Fig.1 X-ray diffraction patterns of as-cast alloys: (a) ZA84; (b) 096Si; (c) 01P

It can be seen from Table 3 that, when silicon is added in ZA84 alloy, the liquidus temperature lowers down, the starting and ending temperatures of ternary phase transformation increase, and the solidification range lessens. When AlP is added in 096Si alloy, the liquidus temperature goes up, the starting and ending temperatures of ternary phase transformation go down a little, and the solidification range increases.

It is worthy to point out that the holding and pouring

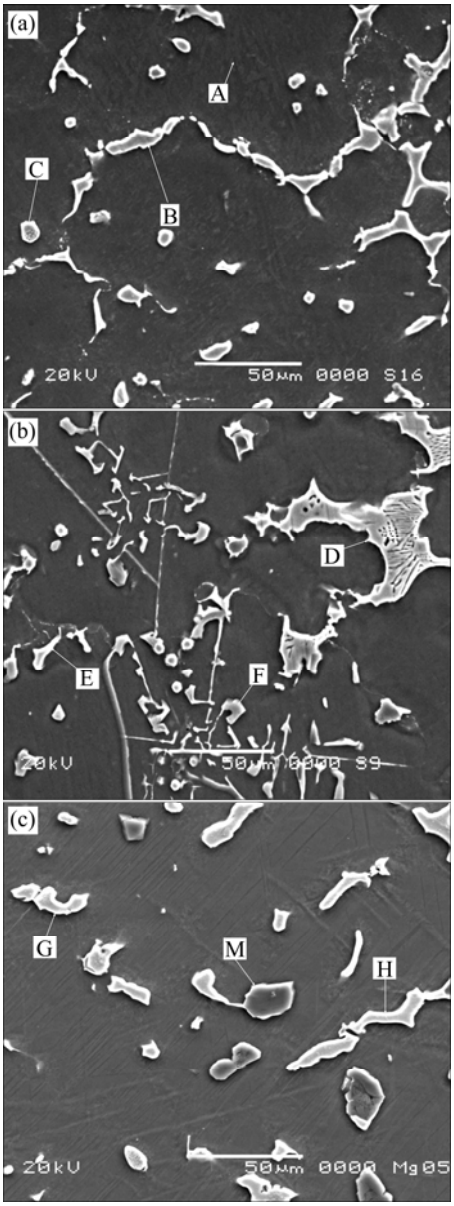

Fig.2 SEM morphologies of alloys: (a) ZA84; (b) 096Si; (c) 01P

Table 2 Chemical composition of spots in Fig.2 by EDXS (molar fraction, %)

Position	Mg	Al	Zn	Si	Phase
A	97.19	1.19	1.62		Mg
B	47.96	18.90	33.14		$\tau(Mg_{32}(Al,Zn)_{49})$
C	56.50	21.25	22.25		$\varphi(Al_2Mg_5Zn_2)$
D	54.15	22.63	23.21		$\varphi(Al_2Mg_5Zn_2)$
E	46.63	15.90	37.46		$T(Mg_{32}(Al,Zn)_{49})$
F	65.12			34.87	Mg_2Si
G	55.86	22.77	21.36		$\varphi(Al_2Mg_5Zn_2)$
H	47.70	11.23	41.06		$\tau(Mg_{32}(Al,Zn)_{49})$
M	66.87			33.12	Mg_2Si

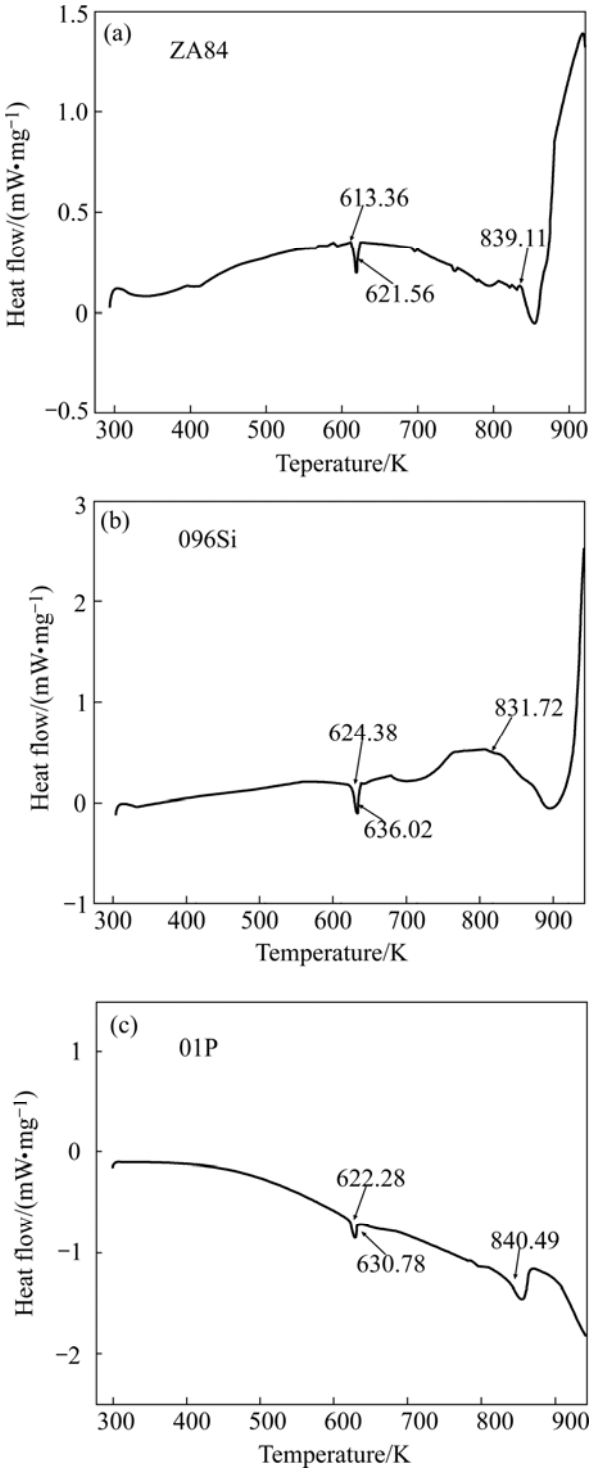

Fig.3 DSC curves of alloys: (a) ZA84; (b) 096Si; (c) 01P (Heating rate 5 K/min)

temperatures of the alloy melt in the course of sample preparation are similar, which are 1 043 K and 1 008 K, respectively. The liquidus temperature of 096Si alloy (831.72 K) is lower than that of ZA84 alloy (839.11 K), and the degree of superheating of 096 Si alloy is larger than that of ZA84 alloy. Therefore, the cooling rate during 096 Si alloy solidification is slower than that of

Table 3 Temperatures of liquidus and ternary phase reactions of alloys

Alloy	Liquidus/K	Phase reaction		Solidification range/K
		Starting temperature /K	Ending temperature (solidus)/K	
ZA84	839.11	621.56	613.36	225.75
096Si	831.72	636.02	624.38	207.34
01P	840.49	630.78	622.28	218.21

ZA84 alloy, which also results from the effect of crystallization latent heat of Mg_2Si. The slow cooling rate results in the reduction of undercooling degree at every stage for phase precipitation during solidification of 096Si alloy. The liquidus temperature of 01P alloy (840.49 K) is higher than that of 096Si alloy, and the degree of superheating of 01P alloy is less than that of 096Si alloy. Therefore, the cooling rate during 01P alloy solidification is faster than that of 096Si alloy, which results in the increase of undercooling degree at every stage for phase precipitation during solidification of 01P alloy.

3.3 Kinetics analysis of phase selection between τ phase and φ phase

Phase selection exists at every stage during solidification. The formation predominance of a phase during solidification depends on its advantageous nucleation or growth rate. In general, phase selection is associated with not only the relative nucleation rate but also the relative growth rate. But when the growth characteristics of two phases are similar, the competition of nucleation rates plays a decisive role in phase selection[8−10].

Because both τ and φ phases have complicated crystal structure, and their growth characters are similar, the phase selection between φ and τ mainly depends on their nucleation condition[11−13]. The mathematical model of heterogeneous nucleation is used to calculate the nucleation rate of τ and φ vs undercooling in the undercooling melt[10,14−15]:

$$J_S=\frac{N_n d_a^2 X_{L,\ eff}(1-\cos\theta)\ D_L\sigma_m^{1/2}}{a_0^4\sqrt{f(\theta)\ R_gT}}\exp\left[-\frac{\Delta G^*}{k_BT}\right] \quad (1)$$

where N_n is the quantity of latent heterogeneous nucleation particles in unit volume melt; d_a is the average atom diameter of nucleation solid phase; $X_{L,eff}$ is the effective alloy concentration[10−16], and its value is always less than 1. $X_{L,eff}$ approaching 1 shows that the composition of solid phase approaches that of the melt. For the binary alloy, $X_{L,eff}=X_{L,A}/X_{S,A}$, when A is rich in crystal nucleus. Here $X_{L,A}$ presents the atom concentration of element A at the solid/liquid interface of crystal nucleus. $X_{L,eff}=X_{L,B}/X_{S,B}$ when B is rich in crystal nucleus. Since the effective alloy concentration of ternary alloy is not available, the average value of the effective alloy concentrations of Zn and Al are used as the effective alloy concentrations of φ or τ. θ is the contact angle of heterogeneous nucleation. D_L is the diffusion coefficient of solute atom in melt, that is

$$D_L=\frac{k_BT\eta(T)}{6d_a} \quad (2)$$

The melt adhesivity $\eta(T)$ is expressed as

$$\eta(T)=10^{-3}\exp[3.34T_L/(T-T_g)] \quad (3)$$

where T_L is the liquidus temperature; T_g is the ideal glass transformation temperature, $T_g=(0.5-0.65)T_L$.

σ_m is the mole solid/liquid interface energy

$$\sigma_m=\alpha\cdot\Delta H_m \quad (4)$$

where ΔH_m is the mole fusion enthalpy, $H_m=T_m\Delta S_m$; T_m is the liquidus temperatures of φ phase and τ phase; ΔS_m is the fusion entropy of compound phase; α_0 is the atom leap distance; R_g is the gas invariance; and T is the undercooling temperature.

There is

$$\frac{\Delta G^*}{k_BT}=\frac{16\pi\alpha^3 f(\theta)}{3R_g}\frac{\Delta S_m}{\Delta T_r^2T_r} \quad (5)$$

where ΔG^* is the critical nucleation energy; k_B is the Boltzmann invariance; a is the solid structural parameter; $T_r=T/T_m$, T_m is the melting point of solid phase; and ΔT_r is the non-dimension undercooling degree, $\Delta T_r=1-T_r$.

The chosen and calculated results of the parameter are given in Table 4. The steady state nucleation rates of τ phase and φ phase in the undercooling melt at a certain temperature can be worked out by combining Eqns.(1)−(5).

Fig.4 shows the relations of τ or φ nucleation rate with temperature in ZA84 undercooling melt. The results indicate that there is a critical degree of undercooling of the melt, and at this critical value, the nucleation rate of τ phase is equal to that of φ phase. If the undercooling exceeds the critical value, the nucleation rate of τ phase is larger than that of φ phase, and τ phase preferentially forms while φ phase is restrained; otherwise, φ phase preferentially forms while τ phase is restrained. The critical degree of undercooling is about 9 K.

The results above indicate that the undercooling degree of 096Si alloy melt is less than that of ZA84, namely, the undercooling degree (relatively to the starting temperature of ternary phase transformation) is less than 9 K when ternary phases precipitate, so φ phase

Table 4 Thermodynamic parameters of alloys

Phase	N_n/cm^{-3}	d_a/m	$X_{L,\,eff}$	α	ΔS_m/(J·mol^{-1}·K^{-1})	A_0/m	θ/(°)
τ	4×10^{16}	2.665×10^{-10}	0.70	0.71	7.27	1.2×10^{-10}	35
φ	3×10^{16}	2.669×10^{-10}	0.78	0.80	8.34	2×10^{-10}	38

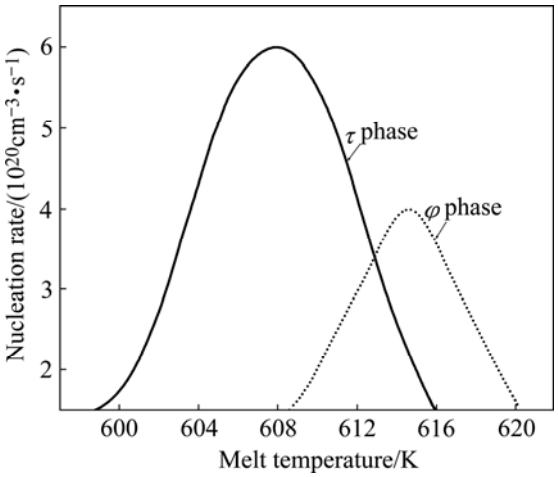

Fig.4 Steady-state nucleation rate of phases τ and φ vs temperature in ZA84 melt

preferentially forms while τ phase is restrained, which brings about the result that the volume fraction of φ phase is larger than τ phase in 096Si alloy. The undercooling degree of 01P alloy melt is larger than that of 096 Si alloy, namely, the undercooling degree (relatively to the starting temperature of ternary phase transformation) is larger than 9 K when ternary phases precipitate, so τ phase preferentially forms while φ phase is restrained, which brings about the result that τ phase is more than φ phase in 01 P alloy.

4 Conclusions

1) φ phase is promoted whereas τ phase is inhibited when silicon is added in ZA84 alloy. The formation of τ phase is facilitated and φ phase is restrained when Al-AlP master alloy is added in 096 Si alloy.

2) The change of the kinetic conditions during solidification results in the phase selection between τ and φ in the alloys.

3) The dynamic process of the phase selections indicates that there is a critical degree of undercooling of the melt. If the undercooling exceeds the critical value, τ phase preferentially forms while φ phase is restrained; otherwise, φ phase preferentially forms while τ phase is restrained. The order of phase selection serves as scientific basis for the selection of strengthening phases in high-zinc magnesium alloys.

References

[1] WANG Li-guo, ZHANG Bao-feng, ZHU Shi-jie, ZHANG Mei, ZHANG Chun-xiang, GUAN Shao-kang. Effects of silicocalcium on microstructure and properties of Mg-6Al-0.5Mn alloy [J]. Trans Nonferrous Met Soc China, 2006, 16(3): 551−555.

[2] SHI Fei, GUO Xue-feng, ZHANG Zhong-ming. Quasicrystal of as-cast Mg-Zn-Y alloy [J]. The Chinese Journal of Nonferrous Metals, 2004, 14(1): 113−116. (in Chinese)

[3] ZHANG Chun-xiang, GUAN Shao-kang, SHI Guang-xin, WANG Li-guo, WANG Jian-qiang, WANG Ying-xin. Microstructure and properties of Mg-8Zn-4Al-1Si-0.3Mn-*x*AlP alloy [J]. The Chinese Journal of Nonferrous Metals, 2004, 14(8): 1353−1359. (in Chinese)

[4] GUAN Shao-kang, ZHANG Chun-xiang, WANG Jian-qiang, WANG Ying-xin, SHI Guang-xin. High zinc magnesium containing silicon and its preparation technique Patent ZL 1 0110192.3 [P]. 2003.

[5] ZHANG Chun-xiang, GUAN Shao-kang, ZHAO Hong-liang. Effects of silicon and AlP on microstructure and properties of Mg-8Zn-4Al-0.3Mn alloy [J]. Materials Science Forum, 2005, 6: 197−200.

[6] ZHANG Z, TREMBLAY R, DUBE D. Microstructure and creep resistance of Mg-10Zn-4Al-0.15Ca permanent moulding alloy [J]. Materials Science and Technology, 2002, 18(4): 433−437.

[7] ZHANG Z, TREMBLAY R, DUBE D, COUTURE A. Solidification microstructure of ZA102, ZA104 and ZA106 magnesium alloys and its effects on creep deformation [J]. Canadian Metallurgical Quarterly, 2000, 39(4): 503−512.

[8] SHAO G, TSAKIROPOULOS P. Prediction of phase select in rapid solidification using time dependent nucleation theory [J]. Acta Metall Mater, 1994, 42(9): 2937−2441.

[9] BA Fa-hai. Phase composition and kinetics study of rapid solidification Ni-Al alloy [D]. Beijing: University of Science and Technology Beijing, 2001: 79−84. (in Chinese)

[10] HU Han-qi. Metal solidification theory [M]. Beijing: China Machine Press, 1999: 24−131. (in Chinese)

[11] SUN W, LINCOLN F J, SUGIYAMA K, HIRAGA K. Structure refinement of (Al, Zn)$_{49}$Mg$_{32}$-type phases by single-crystal X-ray diffraction [J]. Mater Sci Eng, 2000, 294/296: 327−330.

[12] BOURGEOIS L, MUDDLE B C NIE J F. The crystal structure of the equilibrium ϕ phase in Mg-Zn-Al casting alloys [J]. Acta Materialia, 2001, 14(49): 2701−2711.

[13] YUAN Guang-yin, LIU Man-ping, DING Wen-jiang, AKIHISA I. Microstructure and mechanical properties of Mg-Zn-Si-based alloys [J]. Materials Science and Engineering, 2003, A357: 314−320.

[14] FAN Jian-feng, LIU Xin-bao, XIE Hui, WANG Jin-cheng, SONG Guang-sheng, YANG Gen-cang. Phase selection in undercooled melt of Al72Ni12Co16 quasicrystal-forming alloy [J]. The Chinese Journal of Nonferrous Metals, 2003, 13(5): 1088−1091. (in Chinese)

[15] CAHILL J A, GROSSE A V. Homogeneous crystal nucleation in binary metallic melts [J]. J Phys Chem, 1965, 69: 518−522.

[16] DU Wen-wen, SUN Yang-shan, MIN Xue-gang, XUE Feng, WU Deng-yun. Influence of Ca addition on valence electron structure of Mg17Al12 [J]. Trans Nonferrous Met Soc China, 2003, 13(6): 1274−1279.

(Edited by YANG Bing)